## Subproject A5.4

# Optical Biosensors on the Basis of Microdisk Resonators

**Principle Investigator: Heinz Kalt**

**CFN-Financed Scientists: Wolfgang Löffler (1/4 BAT IIa 20 month); M.Hauser (1/2 BAT IIa starting 1.4.2007), Torsten Beck (3/4 E13 1.8.-31.12.2008, 1/2 E13 starting 1.1.2009)**

**Further Scientists: Ch. Sailer, C. Gohn-Kreuz, Ch. Schäfer, T. Großmann, J. Fischer, S. Schleede, D. Flöß, S. Becker**

**Institut für Angewandte Physik**
**Karlsruhe Institute of Technology (KIT)**

**A5.4** Kalt

# Optical Biosensors on the Basis of Microdisk Resonators

## Introduction and Summary

The aim of the project is the realization of photonic sensors on the basis of whispering gallery mode (WGM) resonators for detection of proteins. The main advantages of this approach are the possibility of a highly parallel detection, sensitivity on the few molecule level and the fact that in contrast to other detection schemes the molecules do not have to be labeled.
The detection principle bases on the shift of a resonator optical mode when a molecule gets attached to the resonator. This detection principle has been proven for the case of whispering gallery modes (WGMs) in silica microspheres and microtoroids proposed by S. Arnold (Polytechnic University, New York) and K. Vahalla (CALTECH). The evanescent field of the WGM polarizes a molecule attached to the sphere which in return shifts the resonance frequency of the mode. Single monolayers of molecules and even single molecules can be detected by this very sensitive process. The resonators are functionalized by fixing proteins to its perimeter which then selectively bind to well defined partner molecules as is the case for antigen/antibody combinations or complementary DNA sequences. For the detection of the modal shift of the WGMs an (integrated) waveguide passes a microresonator at a small distance and laser light can couple to a WGM of the resonator if the frequencies match. The transmission spectrum of the waveguide is recorded and the attachment of molecules to a resonator is detected by a shift of the WGM frequencies.
The obvious strength of the microspheres used in [1] is their high Q-factor in the order of $10^6$ when immersed in water, which allows for detection of polarizable molecules with a surface mass density of several 10 pg/mm$^2$. The disadvantage of this procedure is that this method is not easily scalable due to the non-lithographic fabrication method of the microspheres.
An approach which has a larger potential for integration on a chip and for parallel detection of different molecules is based on toroidal microresonators [2]. These resonators also have ultra-high Q-factors and single molecule detection has been proven [3]. The advantage of these resonators is that they can be processed in large arrays. Challenges related to the realization of parallel detection are the coupling of waveguides to many resonators for their readout, the integration with microfluidics for the transport of molecules to the resonators and the integration of a light source on the device.

## 1. Fabrication of whispering gallery mode microresonators

The current project started in November 2006. Currently three PhD-theses (commenced in April 2007, August 2008 and November 2009 respectively) and two diploma theses (both started in November 2010) promote the topic. Six diploma theses have already been completed.

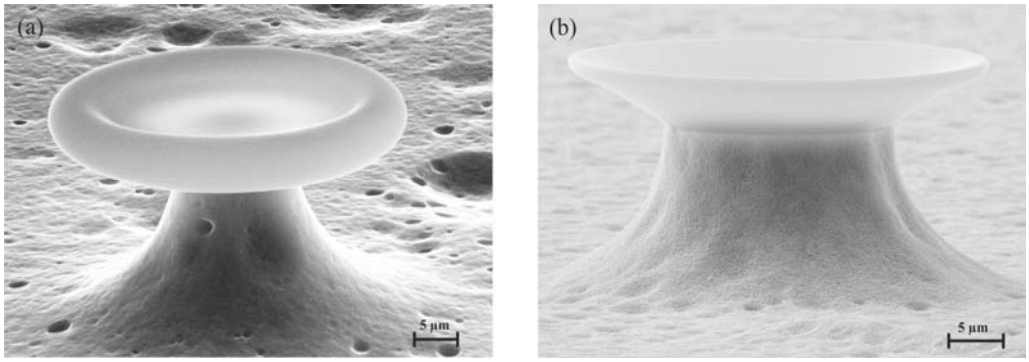

Fig. 1: High-Q (a) toroidal ($SiO_2$) and (b) conical goblet-type (PMMA) microresonator.

Two types of high quality WGM resonators shown in Fig. 1 are available within in the project: silica ($SiO_2$) microtoroids and conical goblet-type resonators made of thermoplastic polymer poly(methyl methacrylate) (PMMA). At the beginning of the project, the necessary techniques for fabrication of high-Q resonators had to be developed. Electron beam lithography, direct writing lithography and UV lithography (strongly using the CFN Z facilities) have been optimized as well as wet chemical etching and reactive ion etching of $SiO_2$ layers. Isotropic etching of silicon substrates without damaging the silica or PMMA resonator structures required the development of a state-of-the-art etching setup based on xenon difluoride ($XeF_2$) located at the CFN clean room. In order to form toroidal silica microresonators with reduced surface quality and highly improved Q-factors, a procedure for selective reflow of $SiO_2$ microdisk structures using a $CO_2$-laser was developed.

As polymer microresonators are essential components for the realization of large-scale and low-cost fabricated photonic devices, we started the development of novel high-Q PMMA resonators with a goblet-type geometry and an ultra-smooth surface. The quality factors amount to $2 \cdot 10^6$ in the infrared and $1 \cdot 10^7$ in the visible spectral region [4].
The PMMA microcavities are fabricated in a four-step process that is applicable for mass production (Fig. 2). In a first step, a 1 µm thick PMMA layer (MicroChem PMMA 950k A7, high molecular weight PMMA dissolved in anisole) is spin coated on top of a silicon substrate. The sample is baked at 110 °C in order to reduce the solvent content. While cooling down the sample, stress is introduced between the PMMA and the silicon substrate due to the difference in the thermal expansion coefficient of both materials. PMMA circles are then directly patterned by UV lithography using deep UV light (=240–250 nm) and a quartz-chromium mask or by electron beam lithography (Fig. 2(a)). For geometrical parameter studies, first samples were fabricated using electron beam lithography. After development (Fig. 2(b)), the exposed silicon substrate is isotropically etched using $XeF_2$, resulting in freestanding PMMA microdisks on silicon pedestals (Fig. 2(c)).

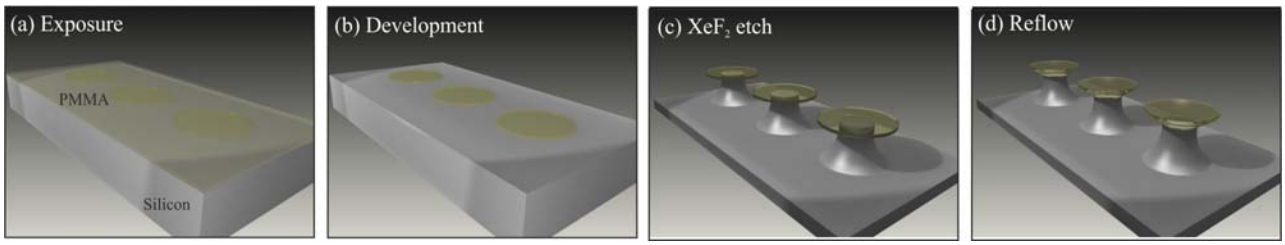


Fig. 2: Process steps for fabricating high-Q goblet microcavities. After exposure (a) and development (b) of PMMA, the silicon substrate is etched using $XeF_2$ (c). A thermal reflow (d) then forms the goblet-type geometry of the cavities.

The measured Q values of these microdisks are above $5 \cdot 10^4$, which is more than a factor of 4 above the Q factors of polymer microdisks published up to now. The dominating loss mechanism is surface scattering caused by the lithographic roughness at the disk periphery, where the WGMs are located. In order to take advantage of the stress in the PMMA layer, a specific thermal reflow step was developed, which allows the reduction of surface roughness and formation of the goblet-type geometry. When the PMMA islands are melted during the reflow process, the liquid photoresist surfaces are pulled into a shape, which minimizes the energy of the system. By heating the sample for 30 s on a hotplate at a temperature of 125 °C slightly above the glass transition temperature of PMMA, heat is transported well defined through the silicon pedestal to the center of the cavity. The temperature of the PMMA, being above the glass transition, allows the surface tension in the PMMA layer to smoothen the cavity surface. In addition, the glass transition state enables the

formation of a goblet resonator by allowing the PMMA surface tension to relax on the upper side of the disk, while the central part of the lower side is fixed by the pedestal. This process is self-quenching, as a further treatment on the hotplate has no effect.

## 2. Characterization

For the task of characterizing the toroidal and goblet resonators, we built up a micro-optics setup. This includes two optical microscopes for optical inspection and alignment of tapered single mode fibers (SMF28) with a diameter of about 1 µm close to the resonator using a five axis positioning stage with a resolution of 20 nm. Measurement of the modal structure and quality factor of the resonators can be performed in the near infrared as well as in the visible spectral region using different single-mode, tunable, external-cavity diode lasers with a small linewidth.
While bringing the tapered section of a fiber close to a resonator, the tunable laser is continuously swept. The transmitted intensity can be monitored using a photodiode. Figure 3 shows a typical transmission spectrum. The laser power is kept below several microwatts in the case of PMMA resonators, avoiding thermal distortion of the resonances, due to field buildup in the cavity and the one order of magnitude larger thermo-optic coefficient of PMMA compared to $SiO_2$.

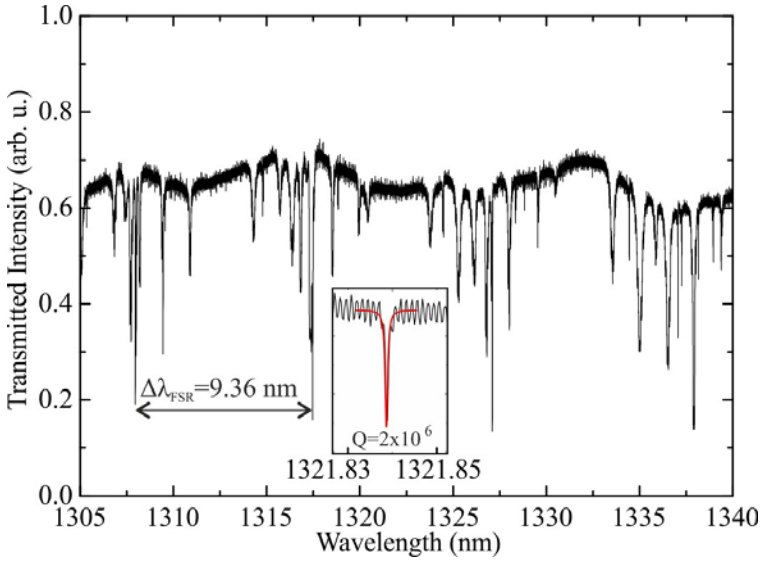


Fig. 3: Transmission spectrum of a tapered fiber optically coupled to a goblet resonator. Taken from [A5.4:2].

## 3. Simulation

For a better understanding of the measured modes and for visualization of the spatial distribution of the excited WGMs in the microcavities, finite element simulations were performed in close collaboration with the Zuse Institut Berlin (ZIB) – DFG-Center Matheon (F. Schmidt). The simulations are performed with the eigensolver JCMResonance (part of the simulation software package JCMSuite developed by the JCMwave GmbH). Computational costs are reduced by taking advantage of the rotational symmetry of the resonator. The eigenvalues (frequencies) are thus computed using cylindrical coordinates in a two-dimensional system by solving Maxwell's equations on a finite number of elements, into which the computational domain is divided (triangulation) before the computation starts.

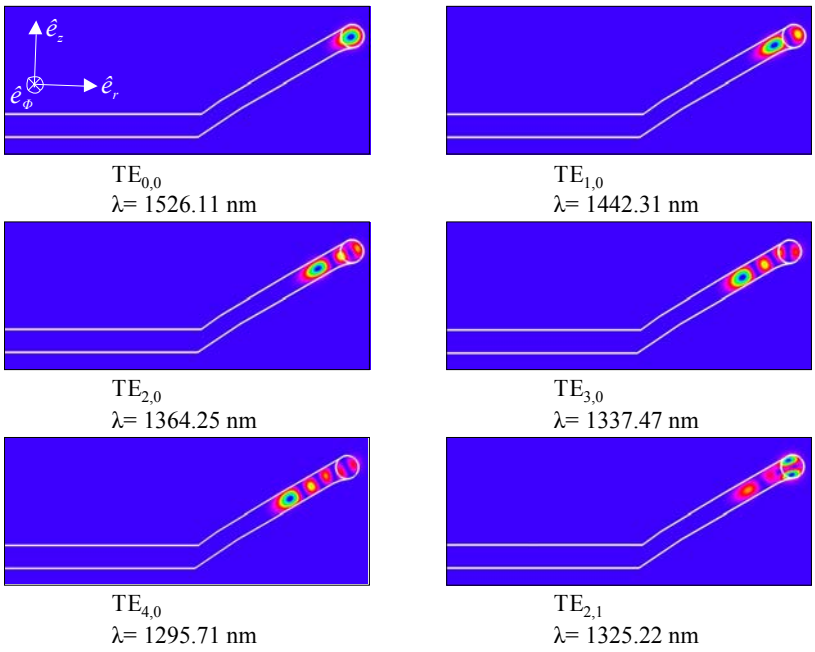


Fig. 4: Simulated mode structure of a goblet microcavity. The intensity distribution and resonance wavelength of the WGMs are calculated. The azimuthal mode number *m* of the presented WGMs is 105.

Figure 4 exemplarily shows the calculated intensity distributions of the $TE_{n,l}(105)$ modes in the goblet microresonators. The spectral positions of the resonances are between 1290 and 1530 nm. The fundamental $TE_{0,0}(105)$ mode is located at the rim of the cavity and has the highest resonance wavelength. As the radial order of the modes increases, the maximum of intensity moves toward the center of the cone. The free spectral range (describing the spectral distance between two adjacent azimuthal modes) was found to be 9.4 nm and perfectly fits to the measured free spectral range denoted in Fig. 3. Comparison of the simulation results with the measurements clearly indicates that the modal structure in the goblet microcavities is dominated by the fundamental mode and higher order radial modes of both polarizations.

In order to study the effect of the tapered fiber on the microresonator's modes and their Q factors, we also performed three dimensional numerical simulations in close collaboration with subproject A5.6 (K. Busch, J. Niegemann and R. Diehl). These classical electrodynamics, full vectorial 3D numerical simulations are performed by applying the Discontinuous Galerkin Time-Domain (DGTD) method [5, 6]. In contrast to the commonly employed Finite-Difference Time-Domain method, the DGTD approach allows for geometry adapted tetrahedral meshes. The setup of the numerical simulation is based on the experimental setup. To simplify the setup slightly, the tapered fiber is modeled as a cylinder of radius 1 μm. Having defined the geometry in a constructive solid geometry manner, the 3D tetrahedral mesh generator "netgen" is applied to generate the mesh, which is depicted in Fig. 5. Sufficiently accurate spatial resolution is ensured by restricting the maximum length of a tetrahedral side to be less than λ/2 in the air filled domain and even smaller in the resonator and the fiber. The resulting mesh contains roughly 500.000 tetrahedra. Mimicking free space at the borders of the computational domain is realized by a combination of perfectly matched layers (PML) and Silver-Müller boundary conditions.

The resonator is excited by a Gaussian pulse centered around 1325 nm, which is launched into the tapered fiber. As DGTD allows the treatment of short pulses, the entire spectral range of interest is investigated with a single simulation run. The transmission spectrum is obtained by two different approaches. First, we record the energy flux through the surfaces at the beginning and end of the fiber, then, a Fourier transform returns the desired spectrum. This approach is time-consuming as

the pulse must circulate roughly Q (factor) times in the resonator. The second approach uses the "harminv" filter diagonalization, which allows the determination of the mode frequencies and their respective Q factors within a short time of simulation.

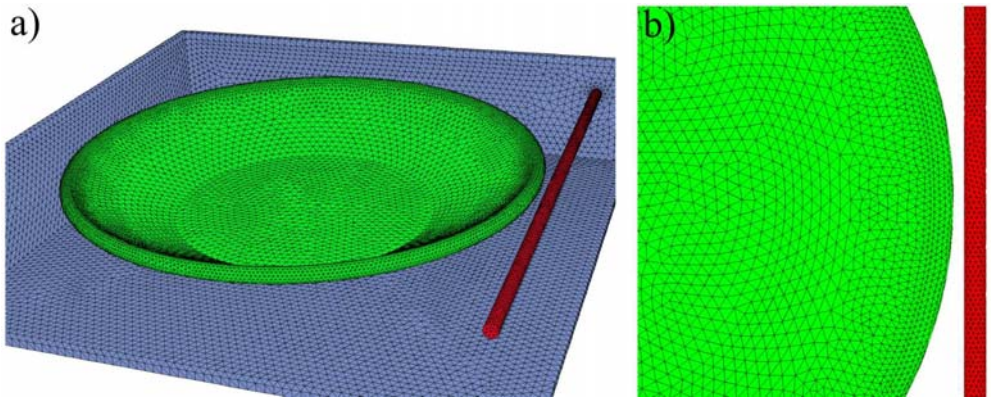


Fig. 5: Three dimensional tetrahedral mesh of (a) the goblet resonator, the tapered fiber and PML regions and (b) the coupling region.

First results show, that the simulated transmission spectra are in good agreement with the measured spectra. More details are given in the report of subproject A5.6. Furthermore, by using this 3D simulation approach, calculation of the shift of the resonance wavelengths due to binding of single molecules will be possible. This could contribute to an ongoing discussion in the literature about the theory of wavelength shifts caused by binding of single molecules to WGM microcavities.

## 5. Biosensing

In order to demonstrate the applicability of the resonators in biodetection we use Bovine Serum Albumin (BSA, molecular weight ≈66.000 g/mol) dissolved in phosphate buffered saline (PBS, pH 7.4). The setup for optical characterization described above was therefore modified. A sample cell was built around the microcones using an aluminum body covered by a glass slide. The solution is retained in the sample cell by surface tension. By using a peltier element in thermal contact with the sample cell, temperature can be controlled precisely. The sample cell is imaged by a charge coupled device camera from above (see Fig. 6(a)).
The sample cell is filled with 200 µl phosphate buffer. The external cavity diode laser is tuned repeatedly from 1302 to 1307 nm and the spectral positions of the dips in the transmitted intensity are tracked using a lorentzian fit. Protein molecules diffuse to the cone's surface from the surrounding buffer medium, are adsorbed and interact with the evanescent field of the WGMs.
Due to the adsorption of the protein, the effective refractive index of the mode changes and the resonance shifts to larger wavelengths. Fig. 6(b) shows the wavelength shift of one optical whispering gallery mode due to absorption of BSA after the injection of the protein. Because of the passivation properties of BSA the shift saturates [7].
The shift can be theoretically estimated by modeling the adhesion of the protein by an increase in diameter of the resonator [8]. The experimentally found shift of the optical mode is about 40 pm, which is in the order of magnitude of the estimation for a 4 nm thick BSA monolayer.

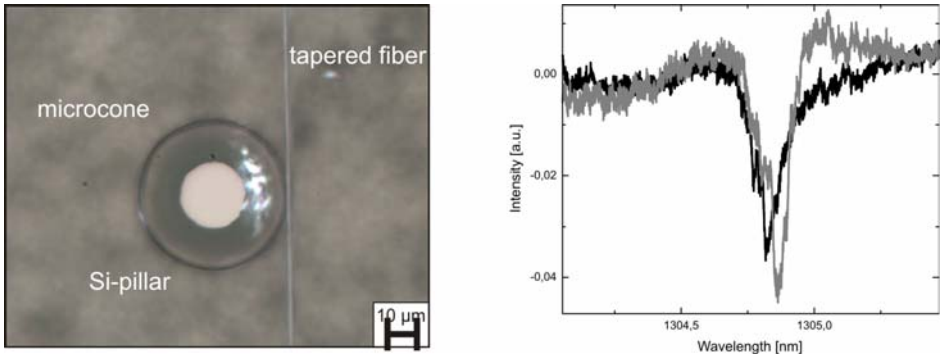


Fig. 6: (a) Picture of a microcone coupled to the tapered fiber. (b) Shift of one whispering gallery mode due to BSA adhesion.

By modifying every goblet resonator on the substrate with substances capable of specific binding to different target molecules a sensor for parallel molecule detection can be realized. Therefore a method for precise depositionof these substances is needed. Two different strategies were pursued. For the rapid coating of single resonators a pulsed droplet spotter [9] was set up (see Fig. 7(a)). As a proof of concept biotin was selectively dropped to a silica surface. Then the whole sample was flushed with a solution of rhodamine labeled avidin. Figure 7(b) shows the local adhesion of avidin caused by the selective binding to biotin.

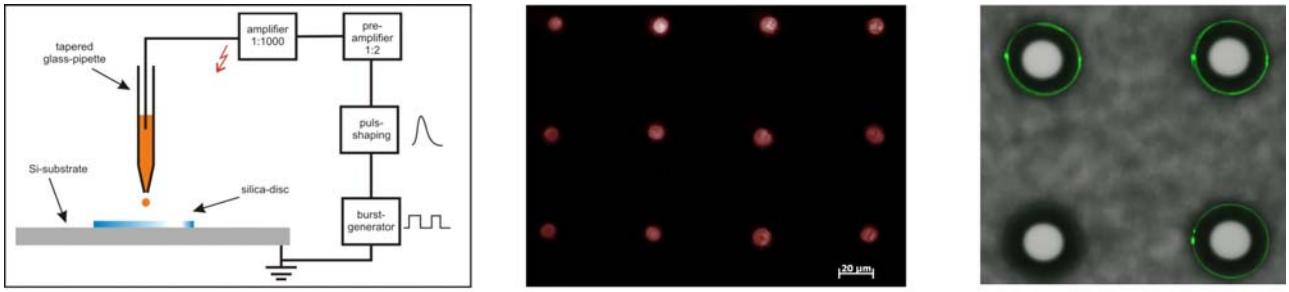


(a) (b) (c)

Fig. 7: (a) schematic drawing of the pulsed droplet spotter: high voltage pulses push the fluid from a tapered capillary to the substrate. (b) This setup allows rapid deposition of femtoliter droplets with micron-resolution. (c) Green labeled phospholipids patterned to the rim of the micro cones.

A slower but more precise method was tested in cooperation with Institute of Nanotechnology (INT, Campus North). The dip pen nanolithography allows deposition of the biological material only on the rim of the resonator. Figure 7(c) shows four cone resonators, three of them are functionalized with phospholipids containing biotin (green labeled) for selective binding to streptavidin. By offering binding sites only on places of maximum interaction with the evanescent field (compare Fig. 4) the limit of detection can be further improved.

## 6. Microcavity dye lasers

For development of narrow-linewidth, coherent light sources which can be integrated on a chip and have low lasing thresholds, WGM microcavities with high Q factors combined with large oscillator strength gain materials are a promising approach. For this, two different ways for integration of gain materials to the goblet microcavities have been developed.

In our first realization, dye molecules such as rhodamine 6G, which are suitable for direct integration in polymeric host matrices, were integrated into the goblet microcavities. This approach allows to create microcavities that may be used as lasers without any additional process steps for their fabrication. Dyes are an efficient gain material with near unity internal quantum efficiency and typically fluoresce at visible wavelengths.
Due to the limited solubility of rhodamine 6G in PMMA, the dye molecules were first dissolved in ethanol and subsequently added to the resist. The resulting concentrations are in the order of several µmol/g solid PMMA. Figure 8(a) shows the obtained spectral absorption and stimulated emission cross-sections for a sample with a concentration of 3.26 µmol/g. The values are in good agreement with measurements obtained for rhodamine 6G in a liquid solution, e.g., in methanol, indicating a small influence of PMMA on the optical properties of the dye. The fabrication of samples with dye-doped goblet microcavities was performed analogue to the case of undoped cavities, described in section 1.
Characterization of polymer lasers is performed in collaboration with A5.5 (U. Lemmer) and in collaboration with Technical University of Denmark (A. Kristensen). The microcavities are optically pumped from above (compare Fig. 8(b)) with 15 ns pulses of a compact, frequency doubled Nd:YAG laser at a pump wavelength of 532 nm and a repetition rate of 5 Hz. Pulsed excitation is used in all measurements to avoid formation of triplets, which quench the fluorescence. The excitation energy is varied using a half-wave plate in combination with a linear polarizer. The output emission is collected with an optical fiber aligned in the plane of the microcavities or alternatively by a microscope objective. The output is then analyzed in a spectrometer.

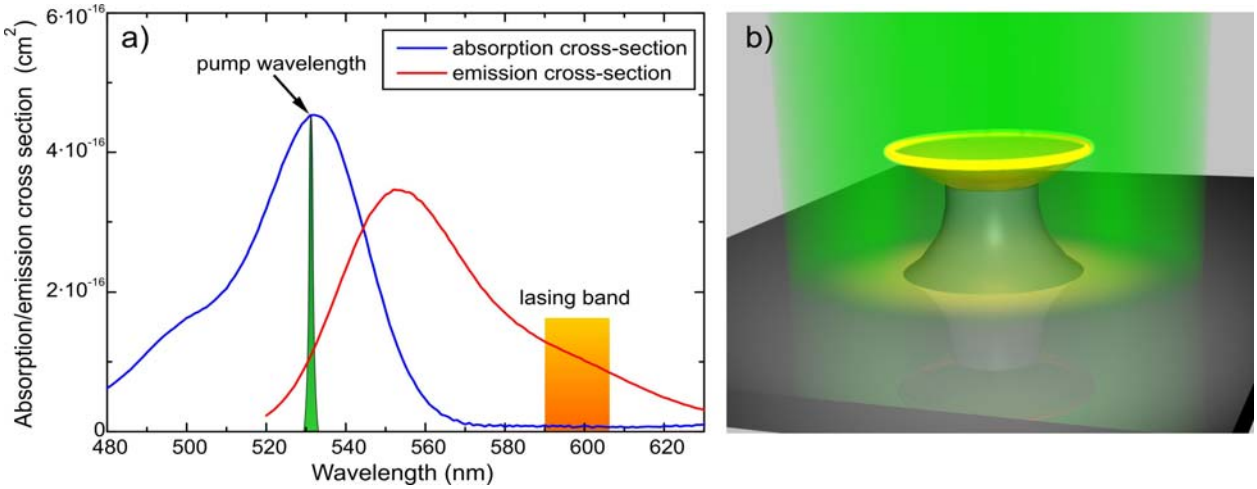


Fig. 8: (a) Absorption and stimulated emission cross-section of rhodamine 6G molecules in a matrix of PMMA. Furthermore, pump wavelength and the spectral region where lasing occurs in the goblet microcavities are indicated. (b) Free space pumping scheme: The microcones are pumped from above at a wavelength of 532 nm and lasing arises in WGMs around 600 nm.

Figure 9 shows data of the measured output emission intensity as a function of the excitation pump energy for a dye concentration of 3.3 µmol/g solid PMMA. The output emission intensity is calculated by integration of emission spectra over single laser lines. The resulting input/output curve has a kink at a pump energy of 3.3 nJ per pulse, demonstrating the low-threshold lasing characteristic of the dye-doped goblet microcavities [10].

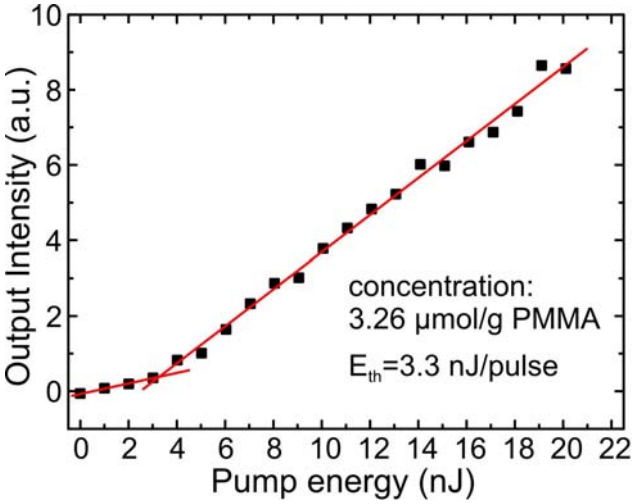


Fig. 9: Input/output curve of a microcone laser (dye concentration: 3.26 µmol/g solid PMMA) with a threshold pump energy of 3.3 nJ per pulse. Taken from [A5.4:5].

In the second approach, developed in collaboration with project A5.5, low-threshold microcavity lasers are fabricated by evaporating a thin film of the organic semiconductor tris(8-hydroxyquinoline) aluminum ($Alq_3$) doped with the laser dye 4-dicyanmethylene-2-methyl-6-(p-dimethylaminostyryl)-4H-pyran (DCM) onto high-Q goblet microcavities. The achieved lasing-thresholds are as low as 1.1 nJ per pulse using free space pumping with emission wavelengths around 650 nm and allow for optical pumping using a low-cost, compact laser diode (Fig. 10).

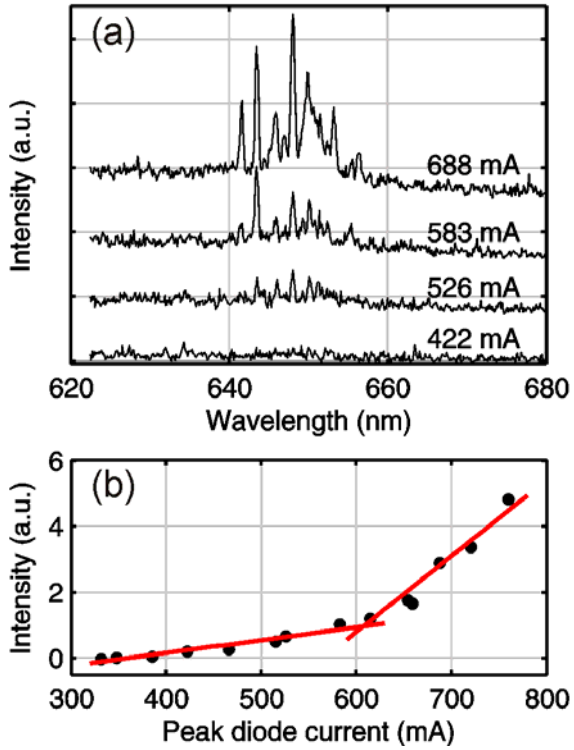


Fig. 10: (a) Emission spectra of the microcavity laser with an $Alq_3$:DCM gain layer at increasing pump energies using the laser diode as pump source. (b) Input/output curve for the microcone laser [11].

As the presented WGM resonators are very sensitive sensor devices, free space laser diode pumped microcavity lasers could provide a step towards compact lab-on-chip sensing systems with the

potential of single-molecule detection. These results have been submitted for publication to IEEE Photonics Technology Letters [11] and a further manuscript is currently in preparation [12].

## 7. Flip-chip approach towards parallel label-free Molecule Detection

Our vision is to combine all the described elements above – microresonators, detection zone, waveguide, light source and an additional microfluidic system – in one device forming a lab-on-chip with the capability of parallel molecule detection. Therefore we successfully applied for start-up financing in the KIT competence field "Matter and Materials" in collaboration with the Institute for Microstructure Technology (IMT) at Campus North. The activities in that area already led to a pending patent application [13].

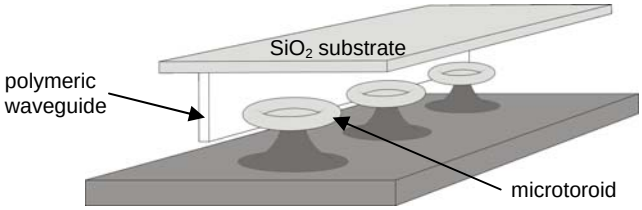


Fig. 11: Schematic drawing of our flip-chip approach. A polymeric ridge waveguide is coupled to many microresonators.

Figure 11 shows a schematic drawing of our flip-chip approach. A polymeric ridge waveguide is processed on a $SiO_2$ substrate. This waveguide is than brought close to a second substrate with many microresonators each functionalized for a specific type of molecule and a microcavity dye laser. This approach allows for easy integration of a microfluidic channel (see Fig. 12) in order to form a lab-on-chip device.

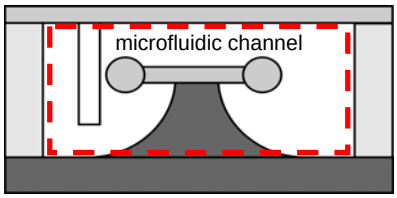


Fig. 12: Integration of a fluidic channel to form a lab-on-chip.

## 8. Public outreach

The activities within project A5.4 have awakened enormous public interest. A scanning electron micrograph of a silica microtoroid served as an eye-catcher at the exhibition "Nano! Nutzen und Visionen einer neuen Technologie", presented by the Landesmuseum Mannheim and Landesstiftung Baden-Württemberg. At the Helmholtz Association's traveling exhibition "Wunderkammer Wissenschaft", started in September 2009 at Berlin's Museum of Technology, several scanning electron micrographs of our structures are presented. Further public interest arouse in the context of the official press release of KIT in August 2010 due to our publication [A5.4:3]. Dozens of web sites published the contents of the press release, among them wissenschaft.de, derStandard.at and pro-physik.de.

## 9. Outlook

In continuation of the here described activities we want to optimize our goblet-type resonators, the methods of functionalization as well as integration of optical and fluidic components to achieve

sensitive bio-sensing devices. In collaboration with the nano-biology projects in project area E we will be able to address problems like detection of DNA sequences. Alternatively one can utilize the sensing capabilities of the WGM resonators for single biomolecule counting.
We further want to use WGM resonators in experiments on cavity quantum electro dynamics (CQED) involving (visible) light. Polariton states result from a strong coupling between cavity photons and single optical emitters like quantum dots lead e.g. to correlation effects between emitted photons (non-classical light). A wide field of new types of photon states opens up, when a coupling of various cavities in chains or arrays is achieved. First results have e.g. been demonstrated for micro-wave photons coupled to superconducting qubits. A most interesting task would be to demonstrate similar CQED effect in the visible or near-IR spectral range. These highly topical effects will be investigated in the new project A6.

**References**

[1] S. Arnold et al., Optics Lett. **28**, 272 (2003)
[2] D.K.Armani, T.J.Kippenberg, S.M.Spillane, K.J.Vahala, Nature **421**, 925 (2003)
[3] A.M.Armani, R.P.Kulkarni, S.E.Fraser, R.C.Flagan, K.J.Vahala, Science **317**, 783 (2007)
[4] T. Grossmann, M. Hauser, T. Beck, C. Gohn-Kreuz, M. Karl, H. Kalt, C. Vannahme, and T. Mappes, *High-Q conical polymeric microcavities*, Appl. Phys. Lett. **96**, 013303 (2010)
[5] J. S: Hesthaven and T. Warburton, Nodal Discontinuous Galerkin Methods (Springer 2008)
[6] J. Niegemann, et al., Photon. Nanostruct.: Fundamentals Appl. **7**, 2-11 (2009)
[7] O. Yogi, et. al., Anal. Chem. **73,** 1896 (2001)
[8] F. Vollmer, S. Armold, Nature Methods **5,** 591 (2008)
[9] B. Sweryda-Krawiec, et. Al., Langmuir, **20**, 2054 (2004)
[10] T. Grossmann, S. Schleede, M. Hauser, M. B. Christiansen, C. Vannahme, C. Eschenbaum, S. Klinkhammer, T. Beck, J. Fuchs, G. U. Nienhaus, U. Lemmer, A. Kristensen, T. Mappes, and H. Kalt, *Low-threshold conical microcavity dye lasers*, Appl. Phys. Lett. **97**, 063304 (2010)
[11] S. Klinkhammer, T. Grossmann, K. Lüll, M. Hauser, C. Vannahme, T. Mappes, H. Kalt, and U. Lemmer, *Diode-Pumped Organic Semiconductor Microcone Laser*, submitted to IEEE Phot. Technol. Lett.
[12] T. Grossmann, S. Klinkhammer, M. Hauser, D. Flöss, T. Beck, C. Vannahme, T. Mappes, U. Lemmer, and H. Kalt, *Strongly confined, low-threshold laser modes in organic semiconductor microcones*, in preparation
[13] T. Grossmann, M. Hauser, C. Vannahme, T. Mappes, T. Beck, and H. Kalt (2010), European Patent No. 09010782.2 – 1524, pending